Postprint of: Grochowska K., Ryl J., Karczewski J., Śliwiński G., Cenian A., Siuzdak K., Non-enzymatic flexible glucose sensing platform based on nanostructured TiO2 – Au composite, Journal of Electroanalytical Chemistry, Vol. 837 (2019), pp. 230-239, DOI: 10.1016/j.jelechem.2019.02.040

Non-enzymatic flexible glucose sensing platform based on nanostructured TiO_2 – Au composite

Katarzyna Grochowska[1], Jacek Ryl[2], Jakub Karczewski[3], Gerard Śliwiński[1], Adam Cenian[1] and Katarzyna Siuzdak[1]

[1]Centre for Plasma and Laser Engineering, The Szewalski Institute of Fluid-Flow Machinery, Polish Academy of Sciences, Fiszera 14 St., 80-231 Gdańsk, Poland

[2]Faculty of Chemistry, Gdańsk University of Technology, Narutowicza 11/12 St., 80-233 Gdańsk, Poland

[3]Faculty of Applied Physics and Mathematics, Gdańsk University of Technology, Narutowicza 11/12 St., 80-233 Gdańsk, Poland

Abstract

All over the world the number of people suffering from diabetes and related complications is drastically growing. Therefore, the need for accurate, reliable and stable sensor for monitoring of glucose in human body fluids is becoming highly desirable. In this work we show that material composed of gold layers deposited onto TiO_2 nanotubes (NTs) formed onto the flexible Ti foil exhibits great response towards glucose oxidation and can be successfully used as electrodes in non-enzymatic and non-invasive electrochemical sensors. TiO_2NTs have been prepared via anodization process followed by calcination at 450°C in order to ensure formation of anatase crystalline phase. Next, gold layers (up to 100 nm) have been deposited on the NTs by means of the magnetron sputtering. The SEM imaging confirmed presence of the well-aligned nanotubes and preservation of their initial architecture after metal deposition for Au thicknesses up to 50 nm. Basing on electrochemical results in the presence of glucose in neutral and alkaline solutions, the optimal Au thickness was found to ensure both the best response and cost-effectiveness. The detection limit of 50 μM and sensitivity of 45 $\mu A/cm^2 mM$ obtained under neutral conditions confirm that prepared material can be used for glucose detection at levels typical for blood, urine or saliva. Moreover, the proposed electrodes exhibit great tolerance to extensive exploitation and multiple bending.

Keywords: TiO_2-Au composite, glucose sensing, electrochemical sensor, non-invasive detection, neutral and alkaline conditions, flexible substrate

1. Introduction

For at least last 10 years the extensive studies to produce functional materials that can be used in non-invasive glucose detection in human body fluids have been conducted. This is of high importance as diabetes is one of the most widespread and lethal diseases in nowadays world and according to World Health Organization by the next 30 years the number of people suffering from diabetes and its complications will rise more than about 60%[1]. It should be underlined that despite many companies and researchers are working on non-invasive glucose monitoring such as by using e.g.: (i) analysis of physiological parameters related to blood sugar in dependence on ultrasound excitation or temperature and electromagnetic field changes (GlucoTrack system)[2]; (ii) GlucoWatch[3]; (iii) lenses with built microsensors[4]; (iv) ionophoretic extraction of glucose from interstitial fluid[5], so far the most reliable method is highly invasive and requires discontinuation of the skin for blood collection. According to Zhang et al.[6], patients puncture themselves at least 1800 times a year which can favor the formation of inflammations at the injection site. Therefore, it is extremely important to continue work on the possibility of controlling the level of glucose in human body through testing fluids other than blood while keeping the accuracy of blood tests. Furthermore, taking into account the glucose level present in other than blood human physiological fluids (e.g. sweat, saliva, interstitial fluid) the linear range of fabricated material for non-invasive detection should fit the range from at least 0.5 mM up to c.a. 7 mM[7].

Most of the sensors developed to estimate glucose level are based on electrochemical measurements, though other methods are also under consideration[8]. Electrochemical sensors can be divided into two categories: non-enzymatic[9] and enzymatic[10,11], which are mainly based on the immobilization of glucose oxidase at the electrode surface. However, the latter suffer from the lack of long-term stability as the enzymes are sensitive e.g. to change of pH or temperature. Therefore, non-enzymatic sensors attracted a lot of attention. Among investigated metallic electrode materials (e.g. platinum[12], palladium[13] or silver[14]), gold is an attractive one due to its high biocompatibility[15,16] and a more negative oxidation potential in neutral and alkaline media compared to the other metals[17]. As it comes to the substrates on which active material can be deposited, glassy carbon[18], indium tin oxide[19], carbon nanotubes[20], titanium dioxide nanotubes[21,22] as well as silica with titanium and graphene layers[23] are considered. Nevertheless, TiO_2NTs are of high interest because of their chemical inertness, resistance to corrosion, biocompatibility and preparation method easily scalable to commercial production. It should be also underlined that most of the investigated substrates are rigid. Therefore, taking into account the possible application under real conditions, many efforts to utilize substrate that exhibit flexibility enabling fit to the body shape are undertaken. For such purposes, some

polyester[24], chitosan composite[25] or some carbon cloth[26] were applied. However, the deposition of an electrochemically active material onto the elastic substrate demands several-step procedure leading to its immobilization and therefore their mass-production is hampered and remains a challenge[27]. Additionally, some bending test proving the activity preservation after the mechanical stress is usually omitted that does not allow for verification of operation in the conditions similar to the real one when the deflection in the place of electrode attachment happens upon time.

In this work, titanium dioxide nanotubes are covered with gold layers via magnetron sputtering and activity of prepared materials towards glucose detection in alkaline and neutral electrolytes is tested. The synthesis method of TiO_2NTs enables formation of the electrode material directly on the substrate and no additional immobilization is required. Scanning electron microscope and X-ray photoelectron spectroscopy performed also under the etching mode are used to determine the surface morphology, penetration depth of gold inside nanotubes and oxidation state of each component present in the electrode material, respectively. Electrochemical characterization of samples confirms possibility of their application in non-enzymatic glucose sensing not only in the proposed solutions of different pH but also in the presence of the human serum. Furthermore, the resistance toward mechanical stress is verified via the multiple bending test combined with activity inspection using cyclic voltammetry technique. Such approach allows to nominate the electrode material for on-body test or other specific applications where elasticity is required. The comparison to other known sensors fabricated with the use of rigid and flexible substrates operating in various environments is also discussed.

2. Materials and methods

2.1. Materials

Titanium foil (99.7%, 0.1. mm thickness) and Au target (99.99%) were purchased from Strem and Quorum Technologies, respectively. Ethanol, acetone, H_3PO_4, ethylene glycol, glucose, ascorbic acid and glycine were bought from Chempur while PBS and NaOH were received from Santa Cruz Technology and POCH, respectively. Human serum type AB (H4522) with glucose concentration of 4.89 mM as well as paracetamol (>99 %) were purchased from Sigma-Aldrich. Deionized water was obtained by means of HLP Smart 2000 (Hydrolab). NaCl (99.5%) and HF (99.9%) were purchased from POCH.

2.2. Sample preparation

TiO_2 nanotubes were prepared via facile anodization process. Before anodization the Ti substrate was cut into 2×3 cm^2 pieces and subsequently cleaned in acetone, ethanol and water bath for 10 min/one solvent followed by drying in the air. The preparation process at 15 V lasted 2 hours in two-electrode system with titanium foil serving as an anode and Pt mesh as a cathode separated at the distance of 2 cm. The electrolyte (V = 100 mL) consists of 6.9 mL of H_3PO_4, 0.65 mL of HF, 30 mL of ethylene glycol and 62.45 mL of H_2O. Then, the titanium plates covered with TiO_2NTs were immersed in 0.05% wt. HF to remove surface debris and rinsed with deionized water. Afterwards, obtained structures were calcinated in 450°C for 2 hours with a heating rate of 2°C/min to ensure the amorphous to crystalline phase transition. In the last step Au layers with different thicknesses up to 100 nm were homogeneously deposited onto prepared samples by means of magnetron sputtering using Q150T S system (Quorum Technologies) equipped with quartz microbalance to ensure control of thickness of metallic films.

2.3. Characterization

2.3.1. Morphology and composition

The surface morphology was examined using the Schottky field emission scanning electron microscopy (FEI Quanta FEG 250) with an ET secondary electron detector with voltage kept at 10 kV. XPS measurements under the etching mode were performed by means of Escalab 250Xi (ThermoFisher Scientific) with a monochromatic Al Kα source. The X-Ray spot diameter was 250 μm and the pass energy 15 eV. The charge compensation was controlled through low-energy Ar^+ ion and low-energy electron emission using a flood gun. The spectroscope was calibrated using Au single crystal. The XPS depth profiling was carried out using Ar^+ ions, bombarding the sample at 30° with a raster width of 1.0 mm. The ion energy was 1000 eV. The etching was carried out for a total time of 5000 s, with various step durations ranging from 50 s at the beginning of the experiment up to 1000 s at its end.

2.3.2. Electrochemical measurements

Electrochemical measurements were carried out using Autolab PGStat 302N electrochemical workstation in three-electrode arrangement where tested material served as working electrode, Pt mesh as counter electrode and Ag/AgCl/0.1 M KCl as reference one. Cyclic voltammetry (CV) tests were conducted in two electrolytes: air-saturated 0.1M PBS and deaerated 0.1M NaOH. The scanning rate was optimized in the range of 10-200 mV/s. Calibration curves were determined by introduction of small portions of glucose into the electrochemical cell and

glucose concentration in electrolytes varied from 0.006 mM to 45 mM. The response of prepared electrodes in the presence of interfering species was measured by adding 0.1 mM of ascorbic acid, glycine and paracetamol. Furthermore, the impact of 0.1 M NaCl was verified since the concentration of the salt in interstitial fluid equals 117 mM and it is assumed to be constant within the physiological range at room temperature[28]. The activity of the TiO_2NTs covered with Au layers under real conditions was checked in the presence of glucose in human serum. The resistance toward the mechanical stress was inspected upon 200 bending cycles accompanied by registration of cyclic voltammograms after each bending route. The bending test was performed by flexing the material in hand to ca. 45°. For completion of the electrochemical characterization the verification of reproducibility with use of 5 different Au-TiO_2NTs electrodes and recurrence upon 50 consecutive measurements for each electrode was performed.

3. Results and discussion

3.1. Morphology and composition of prepared material

It has been previously reported[29,30] that well-aligned and well-ordered TiO_2 nanotubes are formed during anodization process and their geometry (wall thickness, internal diameter, length) strongly depends on preparation conditions such as applied voltage, temperature, time and electrolyte composition[31]. The morphology of top-surface and cross-section of obtained in here titania substrate are shown in Fig. 1. The internal diameter and wall thickness of pristine NTs do not exceed 100 and 20 nm, respectively while the length of nanotubes is estimated to be 580 nm (see Fig. 1 a and b). Deposition of Au layers of thickness up to 50 nm does not lead to filling in the pores (Fig. 1 c) and the electrolyte can easily penetrate them, while for prolonged sputtering (up to 100 nm of Au film) the overgrowing of the NTs can be observed (Fig. 1 d) leading to decrease of the internal diameter of pores. This pattern of Au layer onto TiO_2NTs is consistent with that reported by Zhang et al.[32].

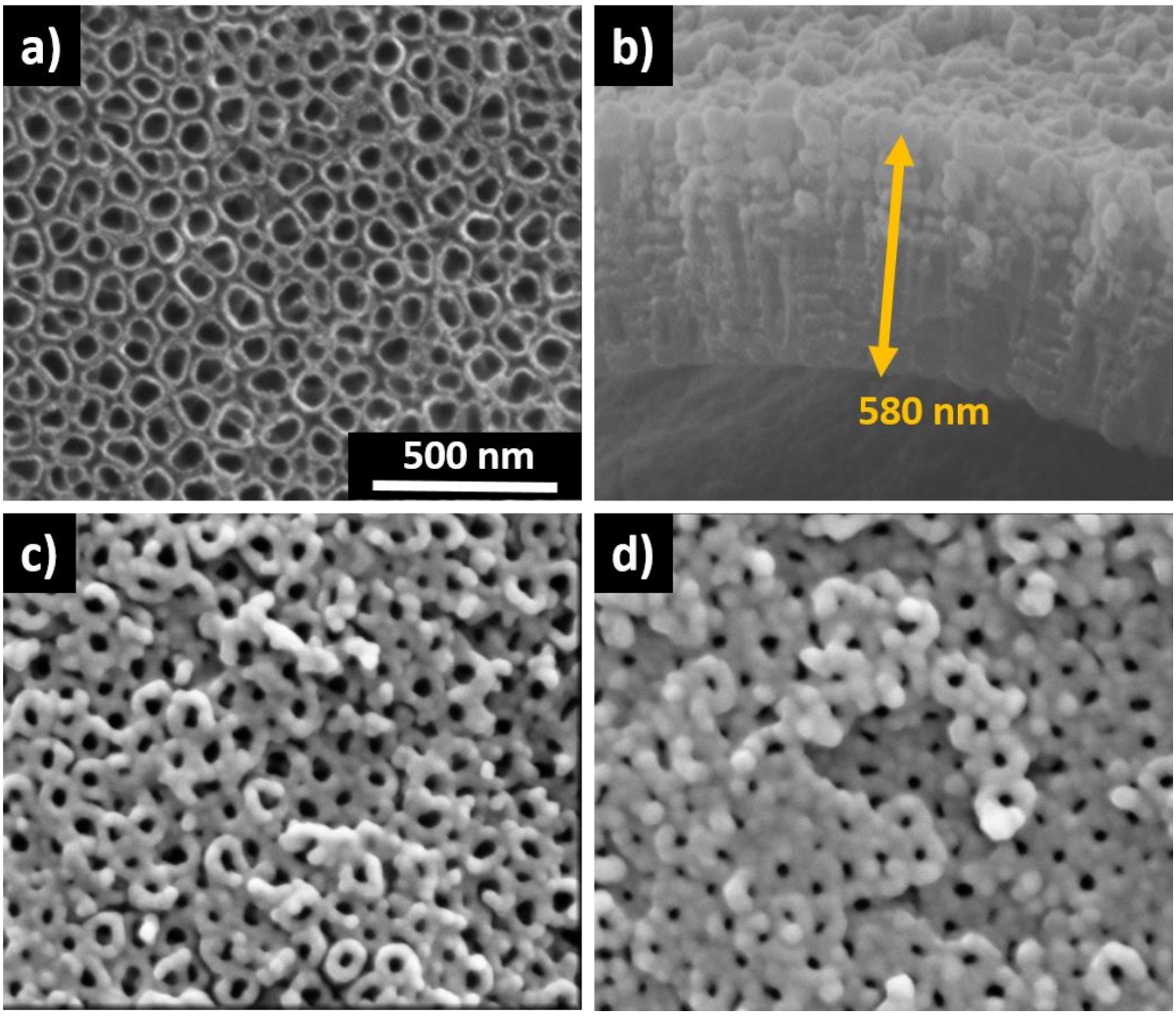

Fig. 1. SEM images of pristine titania nanotubes: top view (a) and cross-section (b) and TiO_2NTs covered with 50 nm (c) and 100 nm (d) Au layers.

In order to inspect the penetration depth of Au inside the nanotube down to the Ti substrate, X-ray photoelectron spectroscopic measurements were performed in a depth profile mode (Fig. 2). The length of titania nanotubes is ca. 580 nm based on data provided from SEM analysis, thus the assumed etching rate of investigated materials is approx. 0.125 nm/s. It has been proven that the presence of gold can be detected down to 200 nm from the surface of the TiO_2NTs toward their base. It can be explained by the formation of the Au collars onto NTs edges (see – Fig. 1 c, d) which prevents the deeper deposition of the metal inside the tubes what is in consistence with observation recorded by Nguyen et al.[33] for Pt.

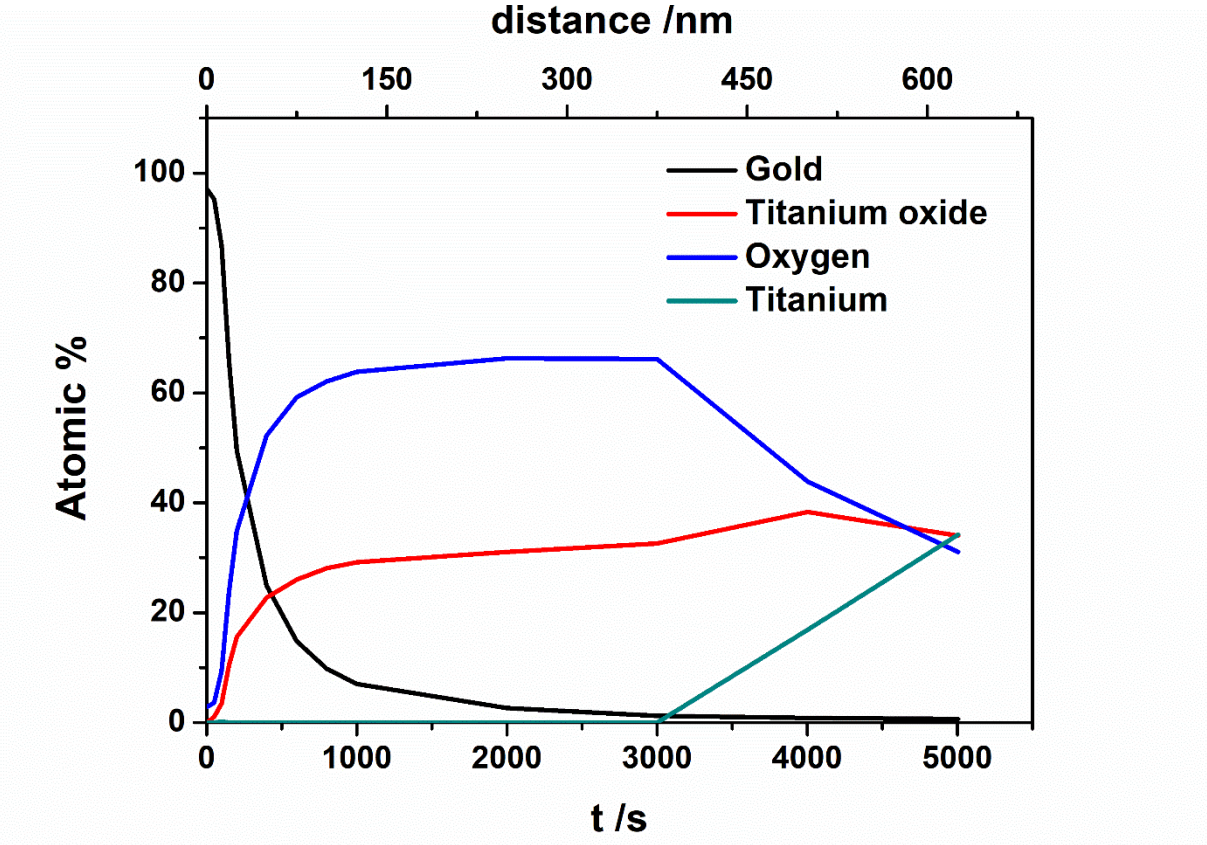

Fig. 2. XPS in depth profile of TiO_2NTs covered with 50 nm Au layer.

Apart from the profile concerning the elemental content, the chemical nature of each element at different depths across the sample was inspected. In general, at the surface area, the photoelectron signal originating from gold is the most intensive and covers those attributed to titanium and oxygen that proves tight coverage of Au film over the tubular substrate. In Figure 3, the spectra registered in the binding energy regime typical for *Ti2p*, *O1s* and *Au4f* were shown. For clarity, values of binding energy for each component used for spectra deconvolution are also given in Table 1. They were recorded at two different etching times: 150 and 5000 s corresponding to the surface and the bulk region of the modified sample, respectively. After first 150 s of etching procedure, XPS spectra for O and Ti are clearly visible. In the case of titanium, the fitting procedure allows to distinguish three types of *Ti2p* doublets assigned to TiO_2, Ti_2O_3 and TiO. The most intensive doublet is attributed to +4 oxidation state whereas peaks typical for +3 and +2 oxidation state of Ti are much weaker[34]. However, as the XPS etching proceeds, the overall contribution of titanium exhibiting +2 and +3 oxidation states increases and near the Ti/TiO_2NTs interface the content of Ti^{+4} reaches the lowest value. The presence of suboxides in titania nanotubes results from the nature of anodization process[35]. According to Petuklov et al.[36], the gradient of oxygen ions appears due to the migration of O_2^-

toward the titanium metallic substrate under the electric field arising during electrochemical oxidation and it leads to the formation of different forms of oxidized titanium. This effect was already confirmed both by transmission electron microscopy and electron diffraction studies.

In accordance with the change in shape of XPS spectra in energy region typical for titanium, the difference in the run of oxygen spectra is observed. At the surface, oxygen signals are weak and along with etching procedure, the spectra registered within binding energy range of oxygen becomes more clear and consist of three singlets with maxima located at 530.8 eV, 531.7 eV and 533.5 eV. According to Yuan et al.[37], the peak at the lowest energy value corresponds to the Ti-O arrangement, while the second one corresponds to the O-C bond[38]. The last one comes from oxygen bonded to hydrogen atom.

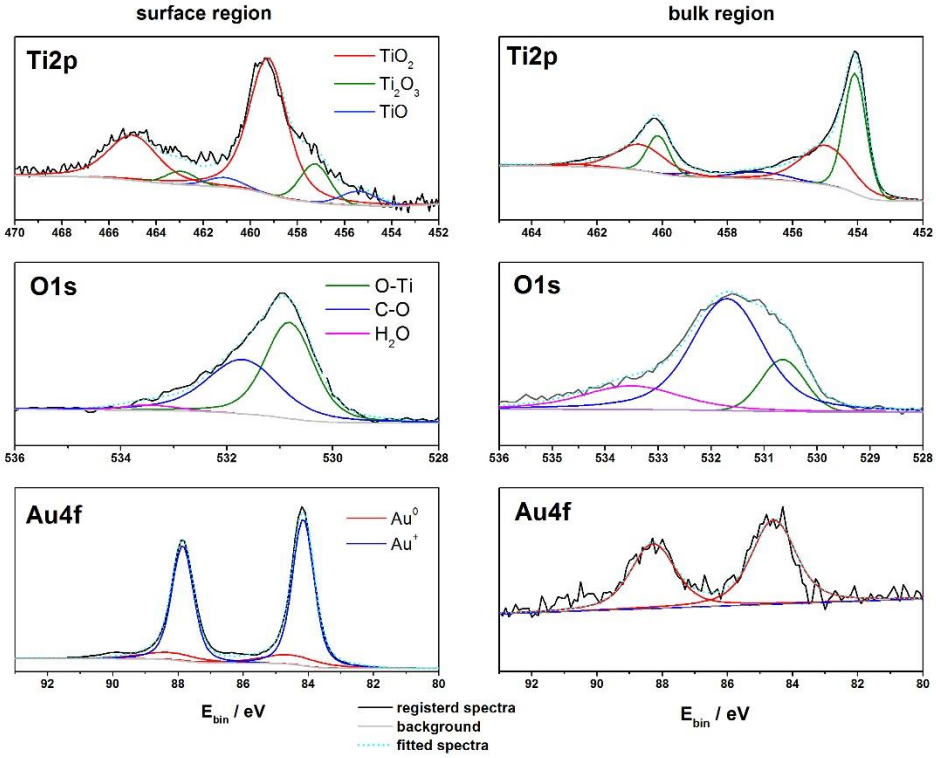

Fig. 3. XPS spectra registered in the binding energy region of titanium, oxygen and gold in the surface region and in bulk of Au-TiO_2NT at different etching times.

Table 1. The binding energy of each component used for XPS spectra deconvolution, accuracy ±0.1 eV.

spectrum	component	binding energy / eV
Au4f 7/2	Au^0	84.1

	Au^{+}	84.6
Ti2p 3/2	Ti^{4+}	459.3
	Ti^{3+}	457.3
	Ti^{2+}	455.4
	Ti^{0}	454.1
O1s	O-Ti	530.8
	OH, C-O	531.7
	H_2O	533.5

In the case of gold, one or two doublets, consisting of signals for orbitals: $Au4f_{5/2}$ and $Auf_{7/2}$, depending on the etching time were proposed for the proper fitting of recorded spectra. The Au^{+}-marked doublet with maxima located at higher binding energy may be assigned to oxidized gold species whereas Au^{0}-labelled signals could be attributed to the metallic gold. Near the surface region, the content of Au characterized with doublet at higher binding energy value prevails that is typical for gold layers deposited onto the surface of some metal oxide substrates[39]. This effect may also result from charging effects under exposure to Ar^{+} ions.
Along with the etching procedure, the atomic content of gold exhibiting maximum of $Au4f_{7/2}$ at 84.6 eV increases. In the certain place of the material cross-section where gold species disappear, the high energy gold phase dominates. Such change in the content of gold phase can be explained by the limited access to oxygen at the deeper material level. As it is usual for titania fabricated via anodization, the signal attributed to carbon was also detected (not included in Fig. 3). The presence of carbon species originates from the graphitic carbon which has been used for the calibration of the XPS spectra[40] and organic electrolyte used for electrochemical oxidation[41]. In the case of anodization used as a synthesis procedure, carbon present in ethylene glycol based solution could be introduced into the titania lattice as an surface dopant.

Summarizing, the results of carried XPS studies show the variable nature of oxidation states of titanium and oxygen as well as their content across the material that results from the dynamics of ion migration occurring during anodization. Modification of TiO_2NTs realized via magnetron sputtering leads not only to the formation of gold film over the tubular edges but also penetration of gold species 200 nm below the titania surface takes place. It makes the surface area of gold/electrolyte interface much greater than in the case of flat electrode, i.e. Au disc and is of great importance for electrochemical activity.

3.2. Electrochemical measurements

3.2.1. Best material selection

Fig. 4 shows cyclic voltammetry curves registered in alkaline and neutral electrolytes containing 5 mM of glucose for TiO_2NTs covered with different thicknesses of Au layers (10-70 nm) as well as for pure titania NTs substrate and gold disc electrode. The discussion about the mechanism of glucose electrooxidation over gold substrate is not the aim of this work and deep analysis for both types of solutions can be found in our previous[8] and other researchers works [42,43].

Briefly, the whole process is initiated via electrochemical adsorption of glucose molecule onto the gold substrate accompanied with dehydrogenation step. The gold oxide film formed in higher anodic potentials exhibits a great catalytic effect on the oxidation of glucose molecules. The adsorbed glucose molecule could be then transformed by a direct oxidation to gluconate and OH^- is released together with H^+ elimination. Other path involves oxidation of dehydrogenated glucose to gamma-gluconolactone followed by transformation to gluconate owing to the reaction with the hydroxide ion. The electrode current is greatly dependent on the glucose concentration and the electrolyte pH (namely amount of OH^-), since OH^- are required to neutralize the protons generated during dehydrogenation stage of the reaction.

Nevertheless, in the case of NaOH only two distinctive peaks appear at +0.2 V and +0.04 V *vs.* Ag/AgCl/0.1M KCl that correspond to glucose oxidation occurring in anodic and cathodic sweep, respectively. It can be observed that for thicknesses below 20 nm the electrodes response is considerably worse in comparison to the flat disc electrode. This can be associated with too small amount of gold as its presence is essential to initiate the process of glucose oxidation at modified titania substrate. For thicker films, when Au thickness exceeds 30 nm, the current density rises drastically. Although glucose oxidation peaks for the prepared material measured in phosphate buffer solution are positively shifted, the similar behavior can be easily seen. It is well known that the presence of OH^- impacts on the CV shape, therefore additional peaks that were not observed for CV obtained in alkaline solution arise.

Overall, for both electrolytes: basic and neutral one, 50 nm Au layer can be considered as adequate compromise between high response and cost-effective amount of gold loading.

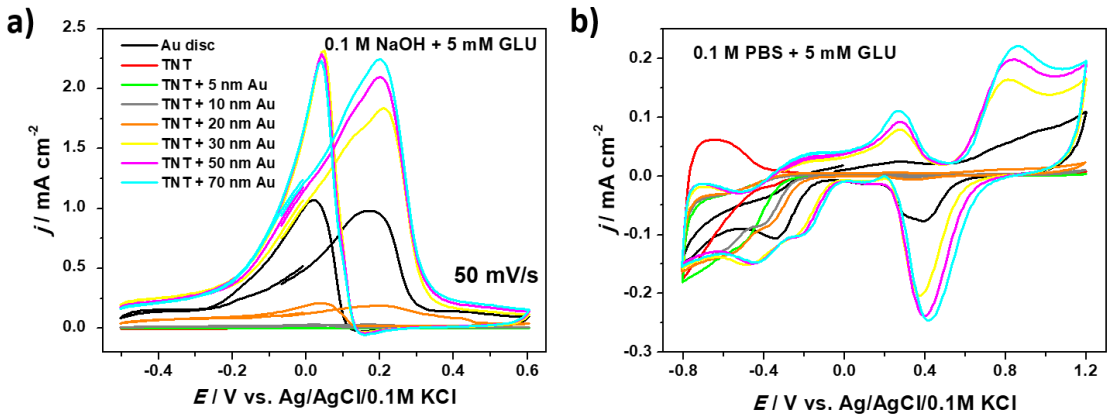

Fig. 4. Cyclic voltammetry of prepared Au-TiO_2NTs materials in 0.1 M NaOH (a) and 0.1 M PBS (b) with addition of 5 mM glucose.

3.2.2. Scan rate effect

Fig. 5 shows cyclic voltammograms of TiO_2NT electrode covered with 50 nm of Au layer measured with different scan rates, in the range of 10-200 mV/s in 0.1M NaOH solution containing 5 mM of glucose. It is clearly visible that oxidation peak located at +0.2 V increases drastically with altered scan rate. Such behavior is related with the size of the diffusion layer and the time taken to register the full scan. Briefly, the voltammogram will be recorded in shorter time when the scanning speed grows up. Thus, the thickness of the diffusion layer will be much thinner in comparison to the slow scan conditions. As the consequence, the flux towards the electrode surface will be higher at fast sweeps than at slower ones. In this case the process is controlled under the diffusion mode since the relation between current density of peak localized at +0.2 V *vs.* Ag/AgCl/0.1M KCl and the square root of the scan rate is linear. However, for the oxidation peak recorded in the cathodic direction, only slight change of current density is observed accompanied with shift towards the negative potential. Similar results have been also reported by Guo et al.[44] and could be related with the concentration of the active sites on the surface and their ability to transfer charge rather than with the thickness of the formed diffusion layer. The sharp shape of the oxidation peak is consistent with the high activity of gold film acting here as a catalyst.

For further electrochemical characterization of the prepared material, the change in the current value of oxidation peak recorded in the reverse scan was taken into account. Therefore, to optimize time of measurements and still maintain the reasonable electrode response, scan rate of 100 mV/s was chosen.

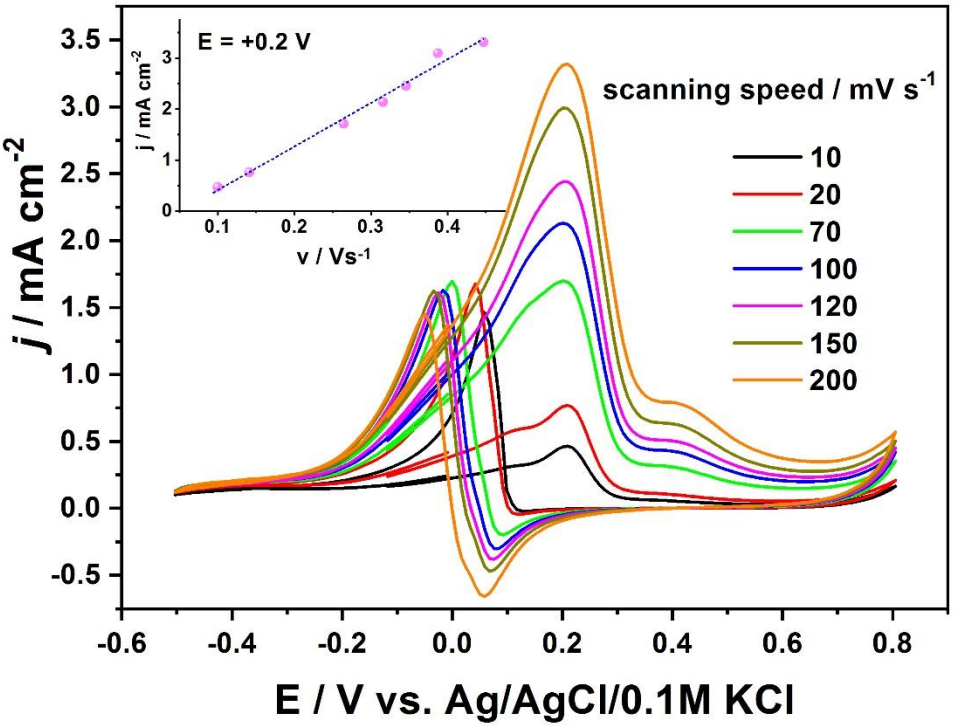

Fig. 5. Cyclic voltammetry curves for 50 nm Au-TiO_2NTs registered in 0.1M NaOH in the presence of 5 mM glucose at scan rates varying from 10 to 200 mV/s, inset: the dependence of the current density of oxidation peak at +0.2 V *vs.* Ag/AgCl/0.1M KCl on the square root of scan rate.

3.2.3. Performance of electrode material

The sensitivity of the best samples among materials with different Au film thicknesses were first characterized by performing measurements in deaerated NaOH solution in different glucose concentration (0.006-45 mM). For clarity, only some examples out of over 30 registered cycles are given in Fig. 6 a. The oxidation peak current density registered in the reverse scan increases gradually with the increasing glucose content in the electrolyte. Basing on the oxidation peak current, the current density versus concentration j *vs.* c relation was graphically shown in Fig. 6 b. A linear relation between glucose concentration and current density is found at the low glucose level (0.05-6 mM) and is characterized by the sensitivity of 540 $\mu A/cm^2 mM$. According to the relation: 3SD/slope, where SD is standard deviation and slope is taken from the linear regression model, the low detection limit of 10 μM was determined. This range corresponds not only to the glucose concentration in blood (3.9-7.1 mM for healthy, non-

diabetics) but also to its levels in other human body fluids such as saliva (0.008-0.21 mM), sweat (0.277-1.11 mM), tears (0.1-0.6 mM)[45] and interstitial fluid in which glucose concentration is two orders of magnitude lower than in blood[5]. Moreover, the linear response can be also observed in the upper concentration range (6-45 mM) with the sensitivity of 185 $\mu A/cm^2 mM$. This relation overlaps with elevated physiological level in blood (up to 11 mM) that can be related to prediabetes states and also with abnormal glucose level (> 11 mM) which is registered for diabetics. It should be underlined that above mentioned diagnostic criteria for blood are set for 2-hour glucose toleration test[46]. When compared to different non-enzymatic glucose sensors tested in alkaline environment for which working parameters are collected in Table 2, the material proposed here shows improved performance both in terms of sensitivity and limit of detection.

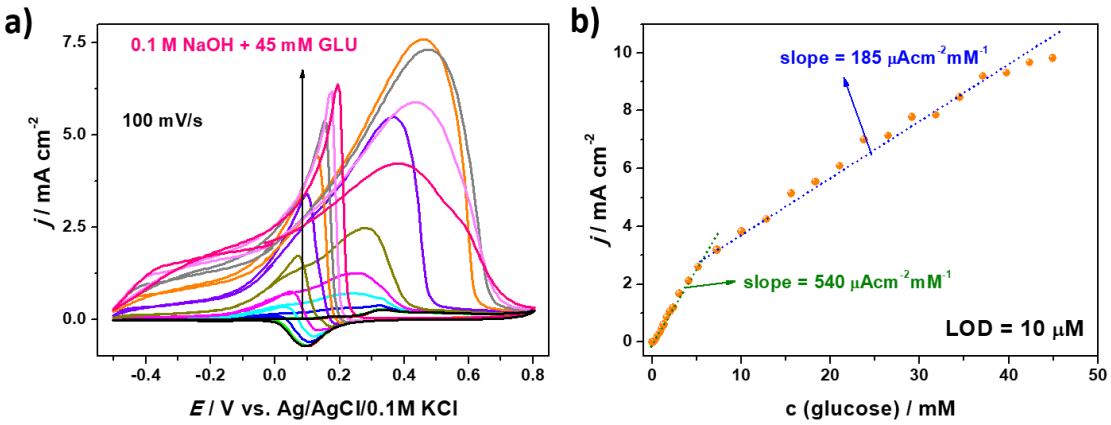

Fig. 6. Electrochemical response of 50 nm Au-TiO_2NTs to successive addition of glucose into 0.1M NaOH (a) and corresponding relation between oxidation current density *vs.* glucose concentration with calibration curve (b).

Table 2. Comparison of working parameters for non-enzymatic sensors operating in basic environment.

material	sensitivity [$\mu A/cm^2 mM$]	detection limit [μM]	linear range [mM]	reference
Au nanodendrites on FTO	37.29	5	0.005-0.06	47
Chitosan-AuNPs on GC	136	370	0.4-10.7	48
Au nanowires on glass	728	30	0.5-14	49
Pt-Au NCs on GC	24.6	3.2	0.2-22	50
Nanoporous Au wires	128.8	8	0.5-10	51
Nanoporous gold film on GC	232	53	1-14	52

Nanoporous gold nanoparticles on Au disc electrode	6.67	0.1	0.1-0.05	[53]
Gold disc	0.72	10	0.5-20	[54]
Porous gold on Au disc electrode	11.8	1	0.01-10	[55]
50 nm Au-TiO_2NTs	540	10	0.05-6	this work
	185		6-45	

The same analysis for the electrode material containing 50-nm thick Au film was performed in the air-saturated 0.1M PBS, and the peak current density registered at +0.4 V *vs.* Ag/AgCl/0.1M KCl was chosen for the investigation of relationship between current and glucose concentration (see – Fig. 7). In this case, the material response can be regarded as linear only in the low concentration range (0.05-3 mM) with the sensitivity of 45 μA/cm^{2}mM and detection limit of 50 μM. Both sensor parameters as well as current density are significantly inferior comparing to the results obtained in NaOH. This can be easily explained by the fact that OH^- ions present in alkaline solution catalases glucose oxidation, and the dehydrogenation process occurs at a slower rate. Additionally, the formation of a more easily oxidized glucose intermediate (enediol) takes place at a faster rate with increased solution pH and the formation of AuOH species highly depends on the OH^- flux transported toward the electrode surface. Nevertheless, prepared electrode is active towards glucose oxidation in neutral solution within the range typical for saliva, tears or interstitial fluids and shows great performance not only in comparison to non-enzymatic sensors but also to the ones modified with enzyme (Table 3). It should be highlighted that verification of Au based materials without attached enzyme is very rarely performed that also raise the value of the proposed enzyme-free sensing material that exhibits the linear response toward glucose level.

All the obtained results suggest that Au-TiO_2NTs can be used in non-invasive glucose sensing and exhibit satisfying sensitivity and limit of detection values both in deaerated alkaline and air-saturated neutral environment. As was also listed in Table 2 and 3, sensing materials are typically fabricated onto the rigid substrate characterized with strictly defined geometric area (Au or GC disc electrode) that limits their on-body usage and other specific applications requiring flexibility.

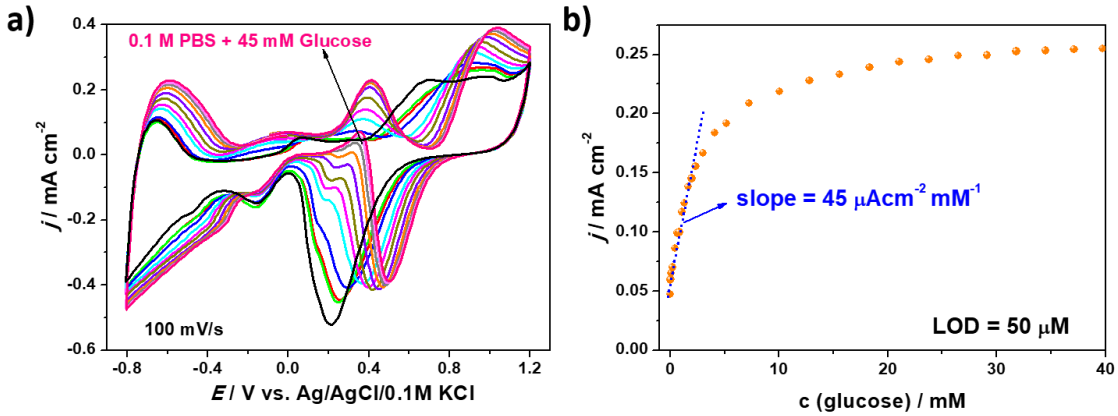

Fig. 7. Electrochemical response of 50 nm Au-TiO_2NTs to successive addition of glucose into 0.1M PBS (a) and corresponding relation between oxidation current density *vs.* glucose concentration with the linear fitting (b).

Table 3. Comparison of working parameters for non-enzymatic and enzymatic sensors operating in neutral environment.

material	sensitivity [μA/cm^{2}mM]	detection limit [μM]	linear range [mM]	reference
non-enzymatic				
Au nanocoral	22.6	10	0.05-30	[56]
Au thin films	18.2	10	0-10	[57]
Au nanotubes	1.13	10	1-42.5	
Pt/CNTs/TiO_2NTs	0.24		0.006-1.5	[58]
AuNPs on graphene paper	52.36	5	0.01-46	[59]
Micro-dual porous gold on screen printed carbon electrode	48.4	25	1.5-16	[60]
Au nanopillar arrays	13.2	60	0.5-9	[61]
50 nm Au-TiO_2NTs	45	50	0.05-3	this work
Enzymatic				
TNT-AuNP/[Demim]Br/Nafion/GOx/GCE	5.1 μAM^{-1}	---	0.01-1.2	[62]
Au/SWCNT/GOx-HRP/PPy/GCE	7.01	30	0.03-2.43	[63]
GOx/CNx-MWCNT/GCE	13	10	0.02-1.02	[64]
Nafion/GOx/4layers of AuNPs/ITO	0.909	2.03×10^3	2-20	[65]

Due to the fact that much enhanced response toward glucose presence is registered for electrode tested in NaOH, further measurements were performed only in alkaline conditions.

However, it should be kept in mind that similar trend in results would be obtained also for neutral solution.

The reproducibility and stability of prepared material were checked by measuring: (i) five different samples of 50 nm Au-TiO_2NTs (Fig. 8 a); (ii) 50 times the same electrode (Fig. 8 b) and (iii) the same electrode exposed to bending test (Fig. 8 c) in the presence of 5 mM glucose. The consistency of results at 95% level confirms that proposed electrodes can be used in long-duration applications and are resistant to the mechanical deformation. Especially, the preservation of the electrochemical activity despite the mechanical stress could be regarded as a key factor for further applications that require flexibility (e.g. on-body, the movable element of some portable device).

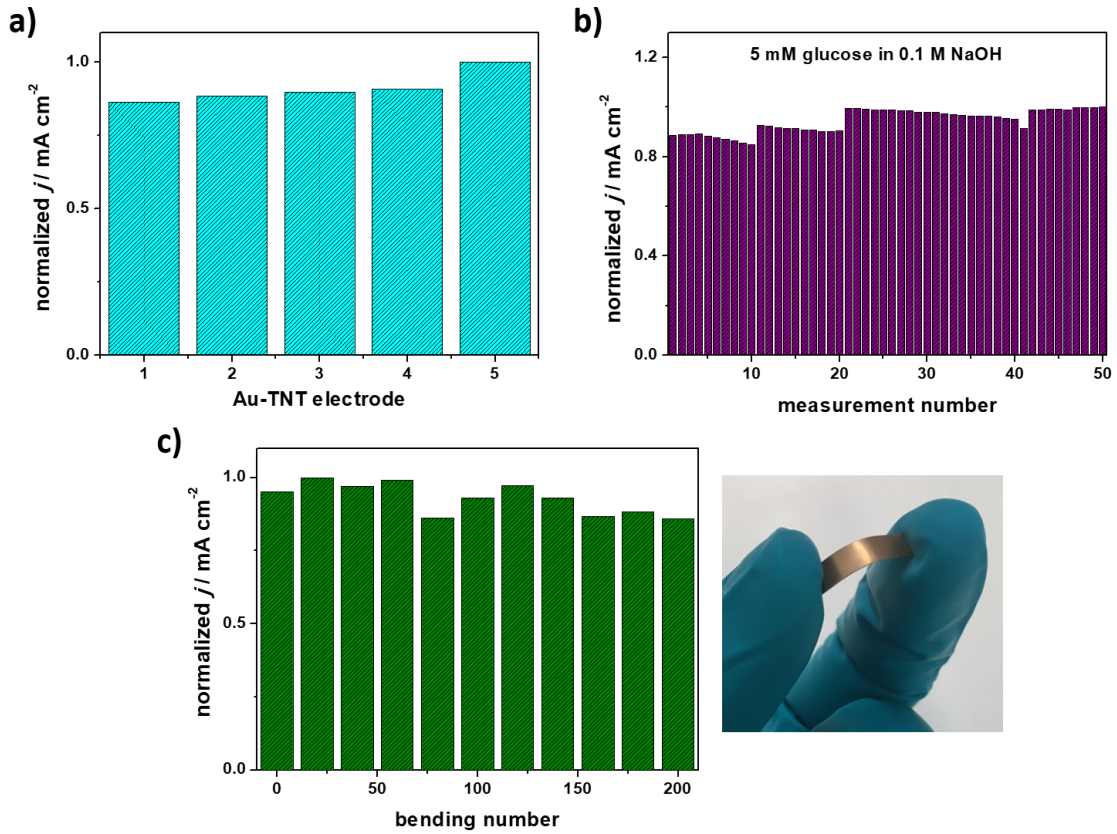

Fig. 8. Reproducibility (a) and stability of 50 nm Au-TiO_2NTs electrode in the case of prolonged measuring (b) and mechanical bending (c) in 5 mM glucose in 0.1M NaOH. Photograph shows the maximal deformation of electrode.

The electrochemical response of the electrode material against different interfering species is shown in Fig. 9. Ascorbic acid, glycine, paracetamol and NaCl were successively added to 5 mM glucose solution. The differences in current density of the oxidation peak registered at 0.04 V for first three substances are negligible. Meanwhile, NaCl strongly

influences the electrode performance. According to Pasta et al.[42] when NaCl is dissolved, the chloride ions can strongly adsorb to the gold active sites leading to the inhibition of the oxidative adsorption of glucose. As a result, decreasing of the intensity of oxidation peak is recorded. This can be overcome by using ion-selective membrane, e.g. Nafion that acts as a barrier layer for anions but is permeable for cations.

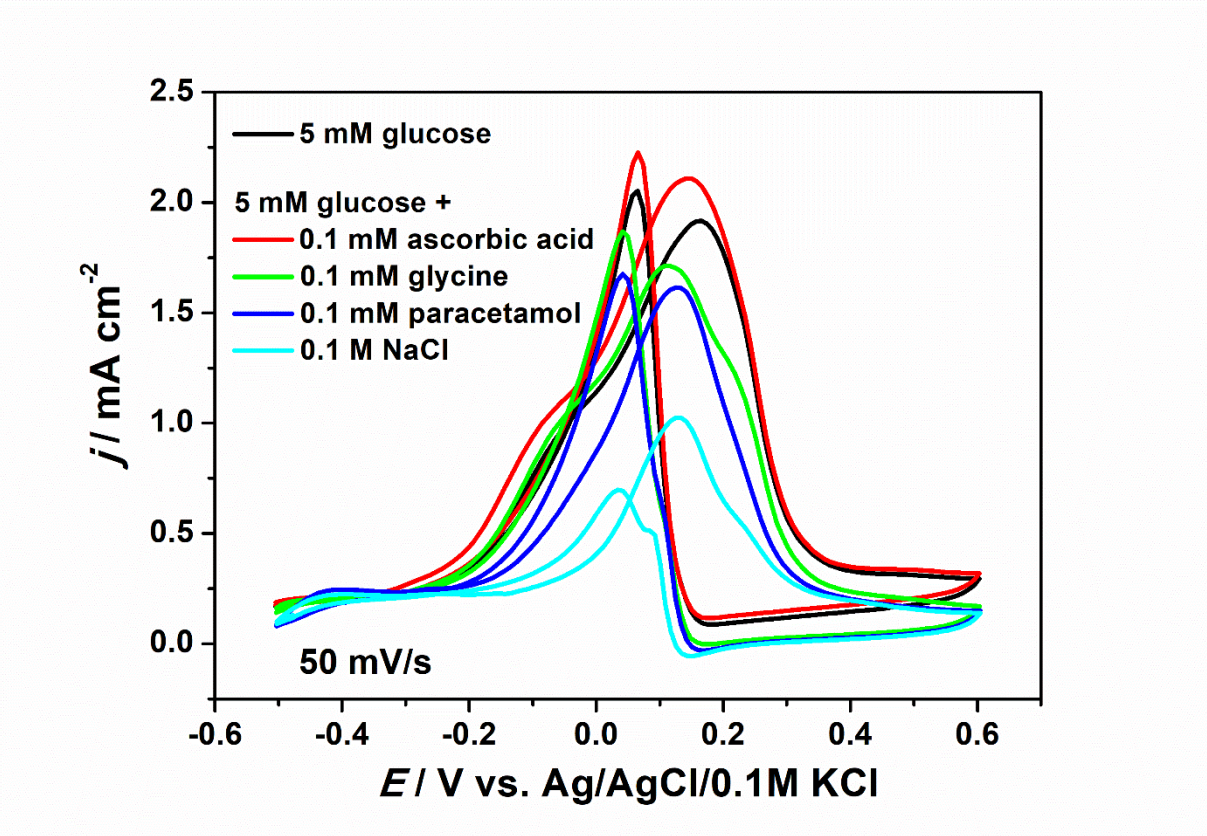

Fig. 9. The influence of interfering species onto the electrochemical response of 50 nm Au-TiO_2NTs.

Finally, the workability of fabricated material was tested in the electrolyte containing human serum. First, 1 ml of human serum was added to 0.1M NaOH electrolyte 3 times and the glucose concentration in the ultimate solution was estimated to be 0.16, 0.3 and 0.4 mM after each addition (Fig. 10 a). To verify the linearity of relationship between the recorded current density and glucose concentration in the low range (i.e. up to 6 mM), different amounts of glucose from the stock solution prepared in alkaline environment were added to the solution of human serum. The linear character of calibration curve (Fig. 10 b) was maintained comparable to the one shown in Fig. 6 b. However, the sensitivity of the electrode decreased to 124 μA/cm^{2}mM and the limit of detection raised up to 50 μM as the current density is noticeably reduced in comparison to measurement performed in the absence of human serum. Such

decrease of material sensitivity is commonly reported[66,67] and it can be ascribed to the presence of proteins fragments in serum which can limit the diffusion of glucose into the electrode surface and its further adsorption. Nevertheless, obtained decrease is much less comparing to nanostructured gold electrode reported recently by Jurik et al.[68] where electrode material exhibits almost 6 time lower activity. It is also worth mentioning that the maxima of oxidation peaks are shifted toward the cathodic regime. This can be explained by above mentioned proteins[69] as well as by the high concentration of chlorides and phosphates that inhibit the electrocatalysis of glucose by competing with OH^- ions[68]. Additionally, the adsorption of glucose to Au surface stays as a rate-determining step of the whole reaction. As it is of common knowledge, glucose exists in two conformations: α and β, wherein β exhibits preferred orientation for adsorption leading to the faster rate of oxidation[70]. In pure alkaline conditions, the α:β ratio equals 20:80 whereas in blood the concentration is regulated by mutarotases and changes to 40:60. Such difference in α:β ratio significantly impacts onto the localization and the value of the oxidation peak. The additional broad band observed at +0.45 V *vs.* Ag/AgCl/0.1M KCl could originate from other species present in blood that could be also easily oxidized at Au surface, e.g. urea.

The reproducibility of electrochemical response of six electrodes towards glucose in human serum was also examined (Fig. 11) and the standard deviation estimated to be less than 2% illustrates very good repeatability and reliability of prepared material.

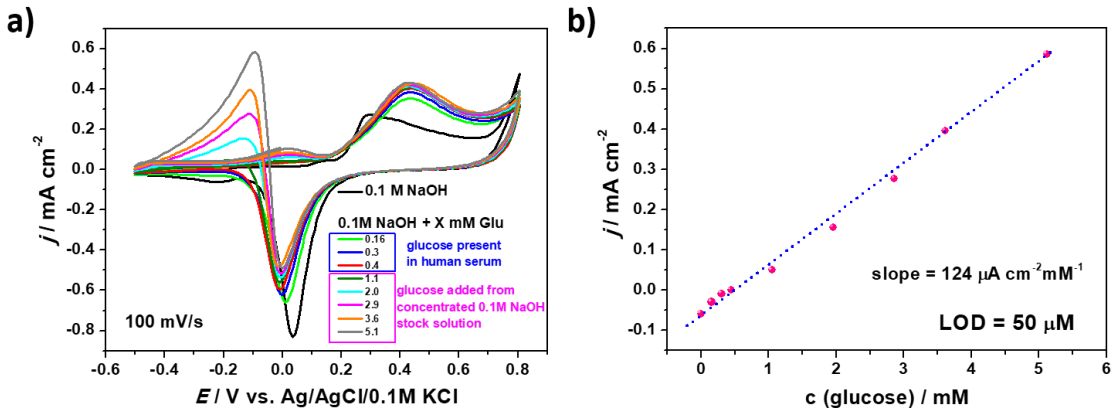

Fig. 10. Electrochemical response of 50 nm Au-TiO_2NTs to successive addition of human serum and glucose into 0.1M NaOH (a) and corresponding relation between oxidation current density *vs.* glucose concentration with calibration curve (b).

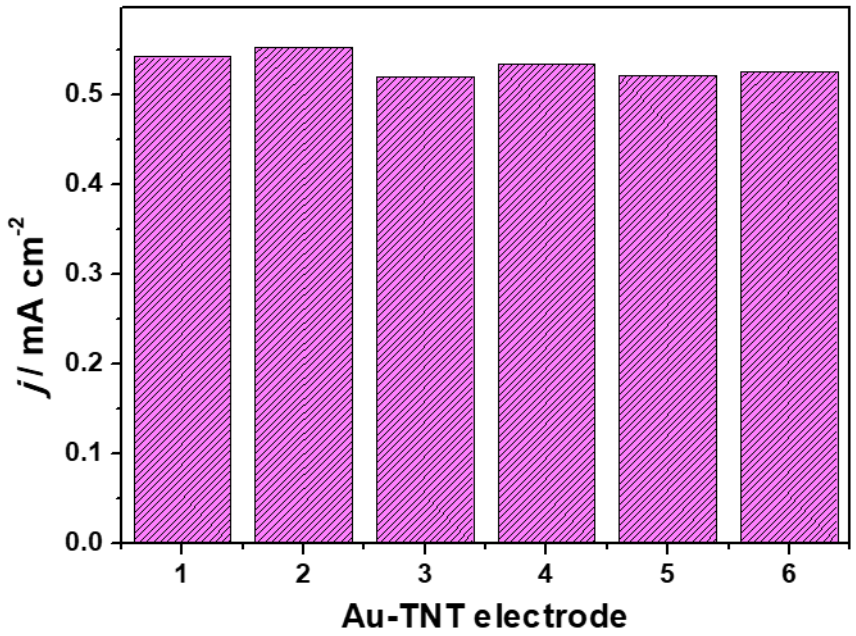

Fig. 11. Reproducibility of 50 nm Au-TiO_2NTs electrode in human serum.

4. Conclusions

In summary, titanium dioxide nanotubes covered with Au layers were fabricated in anodization processed followed by the magnetron sputtering of metal. The as-produced NTs have uniform architecture and structural characterization confirmed the formation of Au collars onto the NTs edges with metal penetration from the surface to 200 nm down the tubes. Electrochemical investigation demonstrates that prepared material can be used as suitable platform for glucose detection both in alkaline and neutral environment. Under the optimized conditions, obtained electrode material exhibits excellent performance towards glucose oxidation giving linear range of 0.05-6 mM and 6-45 mM with sensitivity of 540 and 185 $\mu A/cm^2 mM$, respectively, and low detection limit (10 μM) in NaOH. In the case of PBS, Au-TiO_2NTs array is characterized with the sensitivity of 45 $\mu A/cm^2 mM$ and detection limit of 50 μM with linear range of 0.05-3 mM. Though, the sensitivity for glucose detection in human serum diluted in NaOH drops to 124 $\mu A/cm^2 mM$, presented sensor still satisfies the needs that are required for non-enzymatic sensors operating in normal physiological range for human body fluids. Moreover, gold-titanium dioxide composite provides great stability of results in prolonged measurements and after multiple mechanical deformation. The applied preparation method ensures also the repeatability of morphology of electrodes and can be easily utilized onto commercial scale in applications requiring flexibility and different geometry of the sensing

area. Under investigation are further works to improve the selectivity of the material in terms of interfering species and other sugars present in body fluids.

Acknowledgement

The work is financially supported by The National Centre for Research and Development via grant no LIDER/2/0003/L-8/16/NCBR/2017.

References

[1] http://apps.who.int/iris/bitstream/handle/10665/204871/9789241565257_eng.pdf;jsessionid=A74EDF78E258AC71F97456155A92DFB6?sequence=1 (accessed: 07.08.2018)

[2] http://www.integrity-app.com/the-glucotrack/ (accessed: 07.08.2018)

[3] The Diabetes Research in Children Network (DirecNet) Study Group, Accuracy of the GlucoWatch G2 Biographer and the Continuous Glucose Monitoring System During Hypoglycemia. Experience of the Diabetes Research in Children Network (DirecNet), Diabetes Care 27 (2004) 722-726.

[4] Y. Rim, S. Bae, H. Chen, J. Yan, J. Kim, A.M. Andrews, P.S. Weiss, Y. Yang, H. Tseng, Printable ultrathin metal oxide semiconductor-based conformal biosensors, ACS Nano 9 (2015) 12174-12181. https://doi.org/10.1021/acsnano.5b05325.

[5] A. Bandodkar, W. Jia, C. Yardimci, X. Wang, J. Ramirez, J. Wang, Tattoo-based noninvasive glucose monitoring: a proof-of-concept study, Anal. Chem. 87 (2015) 394-398. https://doi.org/10.1021/ac504300n.

[6] J. Zhang, W. Hodge, C. Hutnick, X. Wang, Noninvasive diagnostic device for diabetes through measuring tear glucose, J. Diabetes Sci. Technol. 5 (2011) 166-172. https://doi.org/10.1177/193229681100500123.

[7] D. Bruen, C. Delaney, L. Florea, D. Diamond, Glucose sensing for diabetes monitoring: recent developments, Sensors 17 (2017) 1866. https://doi.org/10.3390/s17081866.

[8] K. Grochowska, M. Szkoda, J. Karczewski, G. Śliwiński, K. Siuzdak, Ordered titanium templates functionalized by gold films for biosensing applications – towards non-enzymatic glucose detection, Talanta 166 (2017) 207-214. https://doi.org/10.1016/j.talanta.2017.01.075.

[9] M. Guo, P. Wang, C. Zhou, Y. Xia, W. Huang, Z. Li, An ultrasensitive non-enzymatic amperometric glucose sensor based on a Cu-coated nanoporous gold film involving co-

mediating, Sens. Actuat. B: Chem. 203 (2014) 388-395. https://doi.org/10.1016/j.snb.2014.07.007.

[10] F. Kong, S. Gu. W. Li, T. Chen, Q. Xu, W. Wang, A paper disk equipped with Graphene/polyaniline/Au nanoparticles/glucose oxidase biocompatible modified screen-printed electrode: toward whole blood glucose determination, Biosens. Bioelectron. 56 (2014) 77-82. https://doi.org/10.1016/j.bios.2013.12.067.

[11] S. Su, H. Sun, F. Xu, L. Yuwen, C. Fan, L. Wang, Direct electrochemistry of glucose oxidase and a biosensor for glucose based on a glass carbon electrode modified with MoS_2 nanosheets decorated with gold nanoparticles, Microchim. Acta 181 (2014) 1497-1503. https://doi.org/10.1007/s00604-014-1178-9.

[12] Y-H. Wei, C-K. Hsieh, F-G. Tseng, Highly-sensitive non-enzymatic glucose sensor via nano platinum crystals fabricated by phase controlled electrochemical deposition, J. Electrochem. Soc. 165 (2018) B48-B54. https://doi.org/10.1149/2.1141802jes.

[13] R. Ponnusamy, A. Gangan, B. Chakraborty, D.J. Late, C.S. Rout, Improved nonenzymatic glucose sensing properties of Pd/MnO_2 nanosheets: synthesis by facile microwave-assisted route and theoretical insight from quantum simulations, J. Phys. Chem. B 122 (2018) 7636-7646. https://doi.org/10.1021/acs.jpcb.8b01611.

[14] F. Lorestani, Z. Shahnavaz, P. Mn, Y. Alias, N. Manan, One-step hydrothermal green synthesis of silver nanoparticle-carbon nanotube reduced-graphene oxide composite and its application as hydrogen peroxide sensor, Sens. Actuat. B: Chem. 208 (2015) 389-398. https://doi.org/10.1016/j.snb.2014.11.074.

[15] Y. An, Sensitive electrochemical cytosensor based on biocompatible Au@BSA conductive architecture amd Lectin-modified nanoprobe, J. Electrochem. Soc. 163 (2016) B242-B247. http://dx.doi.org/10.1149/2.1091606jes.

[16] J-L. He, Y-F. Tian, Z. Cao, W. Zou, X. Sun, An electrochemical immunosensor based on gold nanoparticle tags for picomolar detection of c-Myc oncoprotein, Sens. Actuat. B: Chem. 181 (2013) 835-841. https://doi.org/10.1016/j.snb.2013.02.063.

[17] M. Tominaga, T. Shimazoe, M. Nagashima, H. Kusuda, A. Kubo, Y. Kuwahara, I. Taniguchi, Electrocatalytic oxidation of glucose at gold-silver alloy, silver and gold nanoparticles in alkaline solution, J. Electroanal. Chem. 590 (2006) 37-46. https://doi:10.1016/j.jelechem.2006.02.018.

[18] X. Kang, Z. Mai, X. Zou, P. Cai, J. Mo, A novel glucose biosensor based on immobilization of glucose oxidase in chitosan on a glassy carbon electrode modified with gold-platinum alloy

nanoparticles/multiwall carbon nanotubes, Anal. Biochem. 369 (2007) 71-79. https://doi.org/10.1016/j.ab.2007.07.005.

[19] K. Grochowska, K. Siuzdak, J. Karczewski, G. Śliwiński, Functionalization of indium-tin-oxide electrodes by laser-nanostructured gold thin films for biosensing applications, Appl. Surf. Sci. 357 (2015) 1684-1691. https://doi.org/10.1016/j.apsusc.2015.10.053.

[20] Y. Yoon, G.S. Lee, K. Yoo, J-B. Lee, Fabrication of a microneedle/CNT hierarchical micro/nano surface electrochemical sensor and its in-vitro glucose sensing characterization, Sensors 13 (2013) 16672-16681. https://doi.org/10.3390/s131216672.

[21] Z-D. Gao, Y. Qu, T. Li, N.K. Shrestha, Y-Y. Song, Development of amperometric glucose biosensor based on Prussian blue functionalized TiO_2 nanotube arrays, Sci. Rep. 4 (2014) 6891. https://dx.doi.org/10.1038%2Fsrep06891.

[22] X. Peng, G. Wan, L. Wu, M. Zeng, S. Lin, G. Wang, Peroxide-like activity of Au@TiO_2 yolk-shell nanostructure and its application for colorimetric detection of H_2O_2 and glucose, Sens. Actuat. B: Chem. 257 (2018) 166-177. https://doi.org/10.1016/j.snb.2017.10.146.

[23] J.C. Claussen, A. Kumar, D.B. Jaroch, M.H. Khwaja, A.B. Hibbard, D. M. Porterfield, T.S. Fisher, Nanostructuring platinum nanoparticles on multilayered graphene petal nanosheets for electrochemical biosensing, Adv. Funct. Mater. 22 (2012) 3399-3405. https://doi.org/10.1002/adfm.201200551.

[24] D. Pradhan, F. Niroui, K.T. Leung, High-performance, flexible enzymatic glucose biosensor based on ZnO nanowires supported on a gold-coated polyester substrate, ACS Appl Mater Inter. 2 (2010) 2409-2012. https://pubs.acs.org/doi/10.1021/am100413u.

[25] X. Xuan, H.S. Yoon, J.Y. Park, A wearable electrochemical glucose sensor based on simple and low-cost fabrication supported micro-patterned reduced graphene oxide nanocomposite electrode on flexible substrate, Biosens. Bioelectron. 109 (2018) 75-82. https://doi.org/10.1016/j.bios.2018.02.054.

[26] M. Xu, Y. Song, Y. Ye, C. Gong, Y. Shen, L. Wang, L. Wang, A novel flexible electrochemical glucose sensor based on gold nanoparticles/polyaniline arrays/carbon cloth electrode, Sens. Actuat. B: Chem. 252 (2017) 1187-11936. https://doi.org/10.1016/j.snb.2017.07.147.

[27] G. Wan, X. Peng, M. Zeng, L. Yu, K. Wang, X. Li, G. Wang, The preparation of Au@TiO_2 yolk-shell nanostructure and its applications for degradation and detection of methylene blue, Nanoscale Res. Lett. 12 (2017) 535. https://doi.org/10.1186/s11671-017-2313-4.

[28] S. Silbernagl, A. Despopolous, Taschenatlas der Physiologie, Thieme, Stuttgart, 2004.

[29] K. Siuzdak, M. Szkoda, J. Karczewski, J. Ryl, K. Darowicki, K. Grochowska, Fabrication and significant photoelectrochemical activity of titania nanotubes modified with thin indium tin oxide film, Acta Metall. Sin-Engl. 30 (2017) 1210-1220. https://doi.org/10.1007/s40195-017-0653-9.

[30] K. Siuzdak, M. Szkoda, A. Lisowska-Oleksiak, K. Grochowska, J. Karczewski, J. Ryl, Thin layer of ordered boron-doped TiO_2 nanotubes fabricated in a novel type of electrolyte and characterized by remarkably improved photoactivity, Appl. Surf. Sci. 357 (2015) 942-950. https://doi.org/10.1016/j.apsusc.2015.09.130.

[31] M. Szkoda, A. Lisowska-Oleksiak, K. Grochowska, Ł. Skowroński, J. Karczewski, K. Siuzdak, Semi-transparent ordered TiO_2 nanostructures prepared by anodization of titanium thin films deposited onto the FTO substrate, Appl. Surf. Sci. 381 (2016) 36-41. https://doi.org/10.1016/j.apsusc.2015.12.126.

[32] W. Zhang, Y. Liu, D. Zhou, J. Wen, L. Zheng, W. Liang, F. Yang, Diffusion kinetics of gold in TiO_2 nanotube arrays for formation of Au@TiO_2 nanotube arrays, RSC Adv. 6 (2016) 48580-48588. https://doi.org/10.1039/C6RA08801E.

[33] N.T. Nguyen, M. Altomare, J.E. Yoo, N. Taccardi, P. Schmuki, Noble metals on anodic TiO_2 nanotube mouths: thermal dewetting of minimal Pt Co-catalyst loading leads to significantly enhanced photocatalytic H_2 generation, Adv. Energy Mater. 6 (2016) 1501926. https://doi.org/10.1002/aenm.201501926.

[34] R.L. Kurtz, V.E. Henrich, comparison of Ti2p core-level peaks from TiO_2, Ti_2O_3 and Ti metal by XPS, Surf. Sci. Spectra 5 (1998) 179-181. https://doi.org/10.1116/1.1247874.

[35] X. Wang, J. Zhao, X. Wang, J. Zhou, Causes for the Formation of Titania Nanotubes During Anodization, IEEE Transaction Nanotechnol. 14 (2015) 113-117. https://doi.org/10.1109/TNANO.2014.2370041.

[36] D.I. Petukhov, A.A. Eliseev, I.V. Kolesnik, K.S. Napolskii, A.V. Lukashin, Y.D. Tretyakov, S.V. Grigoriev, N.V. Grigorieva, H. Eckerlebe, Formation mechanism and packing options in tubular anodic titania films, Microporous Mesoporous Mater. 114 (2008) 440–447. https://doi.org/10.1016/j.micromeso.2008.01.033.

[37] B. Yuan, Y. Wang, H. Bian, T. Shen, Y. Wu, Z. Chen, Nitrogen doped TiO_2 nanotube arrays with high photoelectrochemical activity for photocatalytic applications, Appl. Surf. Sci. 280 (2013) 523. https://doi.org/10.1016/j.apsusc.2013.05.021.

[38] J.H. Xing, Z.B. Xia, J.F. Hu, Y.H. Zhang, L. Zhong, Growth and crystallization of titanium oxide films at different anodization modes, J. Electrochem. Soc. 160 (2013) C239-C246. https://doi.org/10.1149/2.070306jes.

[39] M.P. Casaletto, A. Longo, A. Martorana, A. Prestianni, A.M. Venezia, XPS study of supported gold catalysts: the role of Au0 and Au +d species as active sites, Surf. Interf. Anal. 38 (2006) 2015-2018. https://doi.org/10.1002/sia.2180.

[40] P. Srinivasu, A. Islam, S.P. Singh, L. Han, M.L. Kantam, S.K. Bhargava, Highly efficient nanoporous graphitic carbon with tunable textural properties for dye-sensitized solar cells, J. Mater. Chem. 22 (2012) 20866-20869. https://doi.org/10.1039/C2JM33498D.

[41] J. Zhang, B. Gao, Q. Gan, J. Xia, Y. Cao, J. Wang, K. Huo, Fabrication and capacitive properties of C-doped TiO_2 nanotube array, Chem. Rapid Commun. 2 (2014) 29-32.

[42] M. Pasta, F.L. Mantia, Y. Cui, Mechanism of glucose electrochemical oxidation on gold surface, Electrochim. Acta 55 (2010) 5561-5568. https://doi.org/10.1016/j.electacta.2010.04.069.

[43] L. Zhou, T. Gan, D. Zhang, J. Yan, C. Hu, S. Hu, High-density gold nanoparticles on multi-walled carboion nanotube films: a sensitive electrochemical nonenzymatic platform of glucose, J. Exp. Nanosci. 7 (2012) 263-273. http://dx.doi.org/10.1080/17458080.2010.515253.

[44] L. Guo, Z. Li, K. Marcus. S. Navarro, K. Liang, L. Zhou, P.D. Mani, S.J. Florczyk, K.R. Coffey, N. Orlovskata, Y-H. Sohn, Y. Yang, Periodically patterned Au-TiO_2 heterostructures for photoelectrochemical sensor, ACS Sensors 2 (2017) 621-625. https://doi.org/10.1021/acssensors.7b00251.

[45] P. Makaram, D. Owens, J. Aceros, Trends in nanomaterial-based non-invasive diabetes sensing technologies, Diagnostics 4 (2014) 27-46. https://doi.org/10.3390/diagnostics4020027.

[46] http://www.who.int/diabetes/publications/Definition%20and%20diagnosis%20of%20diabetes_new.pdf (accessed: 22.08.2018)

[47] N.Y. Hau, P. Yang, C. Liu, J. Wang, P-H. Lee, S-P. Feng, Aminosilane-assisted electrodeposition of gold nanodendrites and their catalytic properties, Sci. Rep. 7 (2017) 39839. https://doi.org/10.1038/srep39839.

[48] D. Feng, F. Wang, Z. Chen, Electrochemical glucose sensor based on one-step construction of gold nanoparticle-chitosan composite film, Sens. Actuat. B: Chem. 138 (2009) 539-544. https://doi.org/10.1016/j.snb.2009.02.048.

[49] S. Cherevko, C-H. Chung, Gold nanowire array electrode for non-enzymatic voltammetric and amperometric glucose detection, Sens. Actuat. B: Chem. 142 (2009) 216-223. https://doi.org/10.1016/j.snb.2009.07.023.

[50] Y. Liu, Y. Ding, Y. Zhang, Y. Lei, Pt-Au nanocorals, Pt nanofibers and Au microparticles prepared by electrospinnig and calcination for nonenzymatic glucose sensing in neutral and

alkaline environment, Sens. Actuat. B: Chem. 171-172 (2012) 954-961. https://doi.org/10.1016/j.snb.2012.06.009.

[51] S-H. Su, H. Cheng, P-Y. Chen, Electrochemical oxidation and determination of glucose using cyclic voltammetry and a one-step prepared nanoporous gold wire electrode, J. Chin. Chem. Soc. 60 (2013) 1380-1386. https://doi.org/10.1002/jccs.201300301.

[52] Y. Xia, W. Huang, J.F. Zheng, Z.J. Niu, Z.L. Li, Nonenzymatic amperometric response of glucose on a nanoporous gold film electrode fabricated by a rapid and simple electrochemical method, Biosens. Bioelectron., 26 (2011) 3555-3561. https://doi.org/10.1016/j.bios.2011.01.044.

[53] N. Verma, A green synthetic approach for size tunable nanoporous gold nanoparticles and its glucose sensing application, Appl. Surf. Sci. 462 (2018) 753-759. https://doi.org/10.1016/j.apsusc.2018.08.175.

[54] M. Wooten, J. H. Shim, W. Gorski, Amperometric determination of glucose at conventional vs. nanostructured gold electrodes in neutral solutions, Electroanalysis 22 (2010) 1275-1277. https://doi.org/10.1002/elan.201000006.

[55] Y. Li, Y.Y. Song, C. Yang, X.H. Xia, Hydrogen bubble dynamic template synthesis of porous gold for nonenzymatic electrochemical detection of glucose, Electrochem. Comm. 9 (2007) 981-988. https://doi.org/10.1016/j.elecom.2006.11.035.

[56] T. Cheng, T. Huang, H. Lin, S. Tung, Y. Chen, C. Lee, H. Chiu, (110)-exposed gold nanocoral electrode as low onset potential selective glucose sensor, ACS Appl. Mater. Int. 10 (2010) 2773–2780. http://dx.doi.org/10.1021/am100432a.

[57] M. Gougis, A. Pereira, D. Ma, M. Mohamedi, Oxygen gas assisted laser deposition of gold thin films: electrooxidation of glucose, Int. J. Electrochem. Sci. 9 (2014) 3588–3601.

[58] X.Y. Pang, D.M. He, S.L. Luo, Q.Y. Cai, An amperometric glucose biosensor fabricated with Pt nanoparticle-decorated carbon nanotubes/TiO_2 nanotube arrays composite, Sens. Actuat. B: Chem. 137 (2009) 134–138. https://doi.org/10.1016/j.snb.2008.09.051.

[59] F. Xiao, J.B. Song, H.C. Gao, X.L. Zan, R. Xu, H. W. Duan, Coating graphene paper with 2D-assembly of electrocatalytic nanoparticles: a modular approach toward high-performance flexible electrodes, ACS Nano 6 (2012|) 100-110. https://doi.org/10.1021/nn202930m.

[60] N.X. Viet, M. Chikae, Y. Ukita, Y. Takamura, Enzyme-free glucose sensor based micro-nano dualporous gold-modified screen-printed carbon electrode, Int. J. Electrochem. Sci. 13 (2018) 8633-8644. https://doi.org/10.20964/2018.09.08.

[61] R. Prehn, M. Cortina-Puig, F.X. Munoz, A non-enzymatic glucose sensor based on the use of gold micropillar array electrodes,. J. Electrochem. Soc. 159 (2012) F134-139. https://doi.org/10.1149/2.018206jes.

[62] R. Zhao, X. Liu, J. Zhang, J. Zhu, D. Wong, Enhancing direct electron transfer of glucose oxidase using a gold nanoparticle/titaniate nanotube nanocomposite on a biosensor, Electrochim. Acta 163 (2015) 64–70. http://dx.doi.org/10.1016/j.electacta.2015.02.098.

[63] L. Zhu, R. Yang, J. Zhai, C. Tian, Bioenzymatic glucose biosensor based on coimmobilization of peroxidase and glucose oxidase on a carbon nanotubes electrode, Biosens. Bioelectron. 23 (2007) 528–535. http://dx.doi.org/10.1016/j.bios.2007.07.002.

[64] S. Deng, G. Jian, J. Lei, Z. Hu, H. Ju, A glucose biosensor based on direct electrochemistry of glucose oxidase immobilized on nitrogen-doped carbon nanotubes, Biosens. Bioelectron. 25 (2009) 373–377. http://dx.doi.org/10.1016/j.bios.2009.07.016.

[65] Z.A. Zulkifli, N.S. Ridhuan, N.M. Nor, N.D. Zakaria, K.A. Razak, The Effect of gold nanoparticles modified electrode on the glucose sensing performance, AIP Conference Proceedings 1865 (2017) 020015. http://dx.doi.org/10.1063/1.4993334.

[66] M. Ammam, E.B. Easton, High-performance glucose sensor based on glucose oxidase encapsulated in new synthesized platinum nanoparticles supported on carbon Vulcan/Nafion composite deposited on glassy carbon, Sens. Actuat. B: Chem. 155 (2011) 340-346. https://doi.org/ 10.1016/j.snb.2011.04.016.

[67] M. Gerritsen, J.A. Jansen, A. Kros, D.M. Vriezema, N.A.J.M. Sommerdijk, R.J.M. Nolte, J.A. Lutterman, S.W.F.M. Van Hovell, A. Van der Gaag, Influence of inflammatory cells and serum on the performance of implantable glucose sensors, J. Biomed. Mater. Res. 54 (2001) 69–75.

[68] T. Jurik, P. Podesva, Z. Farka, D. Kovar, P. Skladal, F. Foret, Nanostructured gold deposited in gelatin template applied for electrochemical assay of glucose in serum, Electrochim. Acta 188 (2016) 277-285. http://dx.doi.org/10.1016/j.electacta.2015.12.009.

[69] C. Li, X. Chen, F. Zhang, X. He, G. Fang, J. Liu, S. Wang, Design of cyclic peptide based glucose receptors and their application in glucose sensing, Anal. Chem. 89 (2017) 10431-10438. https://doi.org/10.1021/acs.analchem.7b02430.

[70] F. Largeaud, K.B. Kokoh, B. Beden, C. Lamy, On the electrochemical reactivity of anomers: electrocatalytic oxidation of α- and β-d-glucose on platinum electrodes in acid and basic media, J. Electroanal. Chem. 397 (1995) 261-269. https://doi.org/10.1016/0022-0728(95)04139-8.